

Nuclear Data-Induced-Uncertainty Quantification of Neutron Multiplication Factor and Prompt Neutron Decay Constant for Pb-Bi loaded ADS Benchmark Problems at KUCA

Tomohiro Endo^{1†}, Go Chiba², Wilfred van Rooijen³, Masao Yamanaka⁴, Cheol Ho Pyeon⁴

¹Graduate School of Engineering, Nagoya University: Nagoya, Japan, t-endo@nucl.nagoya-u.ac.jp

²Division of Energy and Environmental Systems, Hokkaido University: Sapporo, Japan, go_chiba@eng.hokudai.ac.jp

³Research Institute of Nuclear Engineering, University of Fukui: Tsuruga, Japan, rooijen@u-fukui.ac.jp

⁴Research Reactor Institute, Kyoto University: Osaka, Japan, {m-yamanaka, pyeon}@rri.kyoto-u.ac.jp

Abstract – By the sensitivity analysis using the SCALE6.2.1/TSUNAMI-3D and the random sampling method using the SCALE6.2.1/Sampler/NEWT/PARTISN, nuclear data-induced uncertainties of neutron multiplication factor k_{eff} and prompt neutron decay constant α are evaluated for Pb-Bi loaded Accelerator Driven System benchmark problems at Kyoto University Critical Assembly. As a result, the nuclear data-induced correlation between α and k_{eff} is strongly negative. It is supposed that the nuclear data-induced uncertainty of subcriticality is major contribution to the uncertainty of prompt neutron decay constant.

I. INTRODUCTION

The Accelerator Driven System (ADS) has been investigated to reduce a burden of nuclear waste disposal by transmuting minor actinides and long-lived fission products. In order to validate nuclear characteristics of ADS, a series of ADS experiments has been conducted at Kyoto University Critical Assembly (KUCA) [1-7]. As one of the ADS experiments, static and kinetic nuclear characteristics were measured for a ²³⁵U-fueled and Pb-Bi-zoned core [7]. The Pb-Bi is considered as a candidate material for the target and the coolant in the designed ADS, thus investigation of nuclear characteristics for Pb-Bi loaded core is important research. For the near critical experimental cores, the neutron multiplication factor k_{eff} was measured using the excess reactivity and the control rod worth. For deep subcritical cores, the prompt neutron decay constant α was measured by the Pulsed Neutron Source (PNS) method using spallation neutrons generated by 100 MeV proton beam from the Fixed-Field Alternating Gradient (FFAG) accelerator [8,9].

The purpose of this study is to numerically analyze k_{eff} and α , and to quantify these uncertainties due to nuclear data for the Pb-Bi loaded ADS experiments at KUCA. By the aid of Uncertainty Quantification (UQ) and Sensitivity Analysis (SA) using the SCALE6.2.1/TSUNAMI-3D, main causes of uncertainty of k_{eff} in this experiments can be clarified [10,11]. The UQ of α is the first attempt, which is achieved by the SCALE6.2.1/Sampler/NEWT [10,12,13] with the PARTISN code [14]. In Sec. II, the target experiments are briefly explained. Then, Sec. III describes the calculation condition and procedure for UQ of k_{eff} and α , followed by the results of Sec. IV. Finally, concluding remarks are provided in Sec. V.

II. EXPERIMENT

The ADS experiments were carried out in the A-core where Highly-Enriched Uranium-Al (HEU) fuel, polyethylene, and Pb-Bi plates were loaded [7]. Figures 1 and

2 shows the core configurations and the loaded fuel assemblies, respectively.

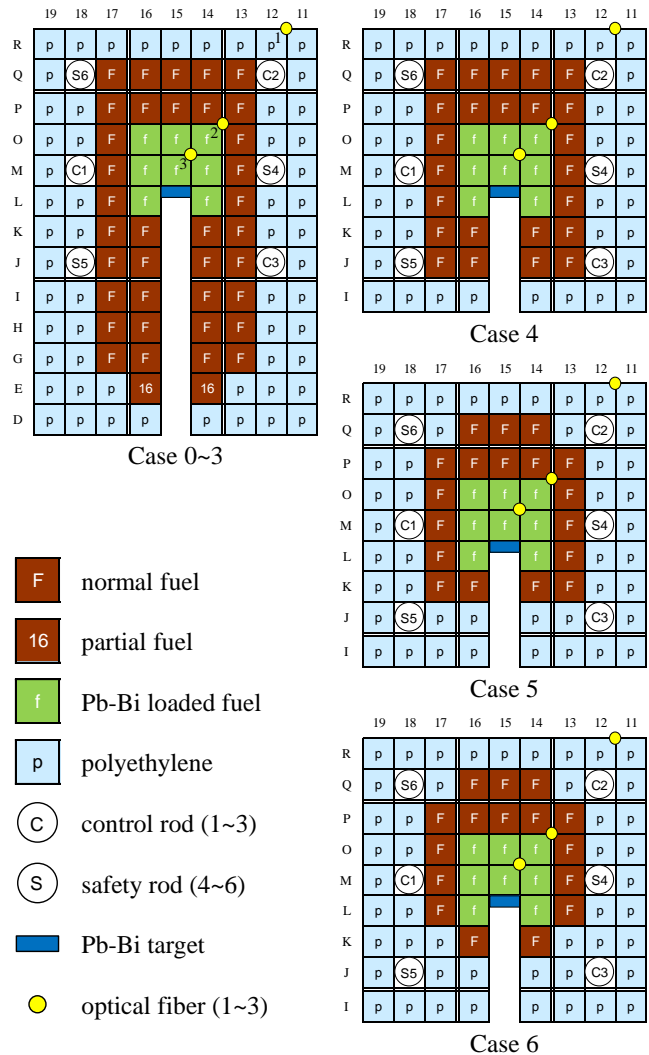


Fig. 1. Top view of Pb-Bi loaded experimental cores.

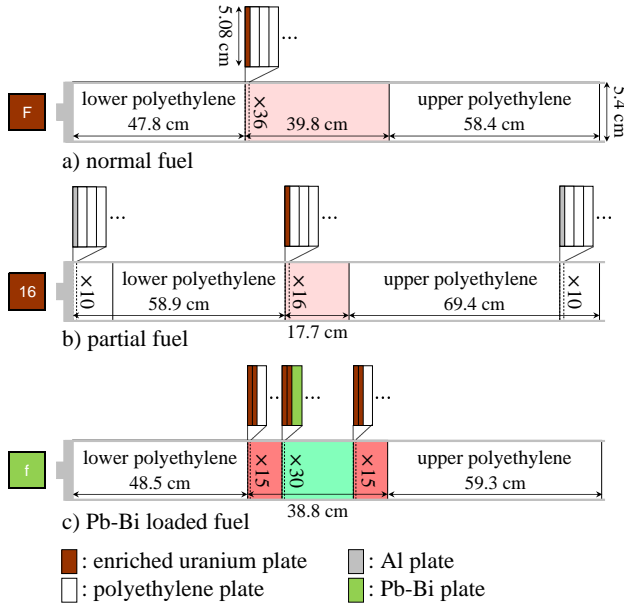


Fig. 2. Fuel assemblies loaded in experimental cores.

There are three types of fuel assemblies. One is a normal fuel assembly “F,” which consists of 36 unit cells (HEU 1/16” thick and polyethylene 3/8” thick). Another is a partial fuel assembly “16,” which consist of 16 times of the same unit cells as “F.” The other is a special Pb-Bi loaded fuel assembly “f,” which consists of total number of 60 unit cells: 30 unit cells for central region (HEU 1/8” thick and Pb-Bi ~3.3 mm thick) and other 15+15 unit cells for upper and lower regions (HEU 1/8” thick and a polyethylene 1/8” thick).

As shown in Fig. 1, there are 7 cases of experimental cores by changing the number of “F” assemblies and the following control rod patterns:

- Case 0: Critical state by C2 rod, other rods withdrawn
- Case 1: C1, C2, C3 inserted; S4, S5, S6 withdrawn
- Case 2: C1, C2, C3, S5 inserted; S4, S6 withdrawn
- Case 3: All rods inserted
- Cases 4~6: All rods withdrawn

The subcriticality $-\rho = (1 - k_{\text{eff}})/k_{\text{eff}}$, which is the absolute value of negative reactivity ρ , for Cases 1~3 was deduced using (1) the excess reactivity by the positive period method and (2) the control rod worth by the rod-drop method [15]. In order to convert the dollar unit of subcriticality to the $\Delta k/k$ unit, the effective delayed neutron fraction β_{eff} for each of experimental cores was evaluated using the MCNP6.1 [16] with the JENDL-4.0 [17].

On the other hand, the subcriticality for Cases 4~6 was not directly measured by the positive period and rod-drop methods, since Cases 4~6 were too deep subcritical systems to reach the critical state for the positive period and the rod-drop methods. For these deep subcritical cores, the prompt neutron decay constant α was measured by the PNS method, where the spallation neutrons were generated by the combination of the FFAG accelerator and the solid Pb-Bi target. The main characteristics of proton beams were as

follows: 100 MeV energy, 1 nA intensity, 20 Hz beam repetition, and 50 ns beam width. In the PNS method, three optical fiber detectors (#1~3 in Fig. 1) were used to obtain the time variation of neutron count rate [18].

III. NUMERICAL ANALYSIS

1. Uncertainty quantification of k_{eff}

The nuclear data-induced uncertainties of k_{eff} (denoted as s_k) were evaluated using the SCALE6.2.1/TSUNAMI-3D. In the TSUNAMI-3D, continuous energy Monte Carlo calculation was performed by the KENO-V.a [19] with the ENDF/B-VII.1 library [20]. As an example, Fig. 3 shows the calculation geometry for Case 6. The CLUTCH method was used for the SA to reduce computational memories [11]. The neutron histories per generation (npg), total number of generations (gen), and skip generations (nsk) are 40000, 5400, and 400, respectively. In the CLUTCH method, $F^*(\vec{r})$ meshes, which are used for adjoint weighted tallies for SA, were spatially divided by approximately $1 \times 1 \times 1$ cm cell units for fuel regions. As a covariance of nuclear data, 56 group covariance library (56groupcov7.1) was used.

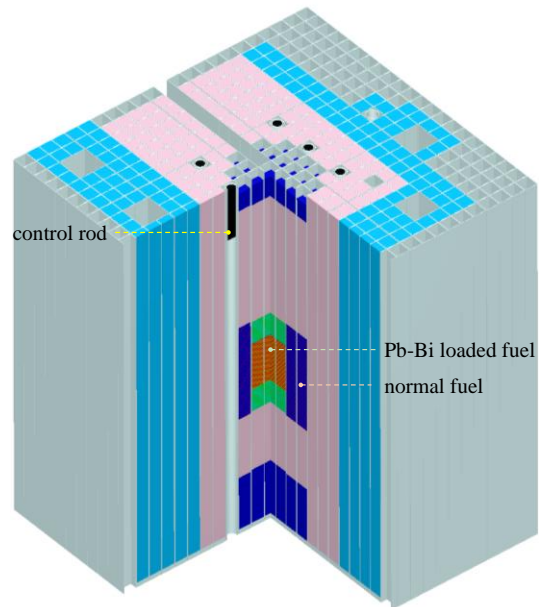


Fig. 3. Slice view of calculation geometry in the TSUNAMI-3D (Case 6).

2. Uncertainty quantification of α

For deep subcritical cores (Cases 4~6), the prompt neutron decay constant α was measured by the PNS method. These measurements values are useful for the validation of prompt ω -eigenvalue calculation. For example, deterministic neutron transport codes such as the DANTSYS [21] and the PARTISN [14] have a function to search the “time absorption” eigenvalue. In this section, the calculation procedures for UQ of α are explained.

A. Theory of ω -eigenvalue Equation

In a strict sense, the prompt neutron decay constant α corresponds to the most negative eigenvalue of spatial and energetic fundamental mode for the natural ω -eigenvalue equation, which includes not only prompt but also delayed neutron production effects [22,23] (Note that α is defined by $-\omega$ in this paper):

$$\frac{\omega}{v_g} \psi_g = \left(-\mathbf{A} + \mathbf{F}_p + \sum_{i=1}^6 \frac{\lambda_i}{\omega + \lambda_i} \mathbf{F}_i \right) \psi_g, \quad (1)$$

where ψ_g and v_g are neutron flux and velocity of g th energy-group; \mathbf{A} , \mathbf{F}_p , and \mathbf{F}_i are net loss (leakage and net absorption), prompt neutron production, and i th precursor-group delayed neutron production operators, respectively; λ_i is the decay constant of i th precursor. Let us consider about a deep subcritical state and/or a harder neutron spectrum such as $\alpha > 1000$ [1/sec]. Then, since $\alpha \gg \max(\lambda_i) \approx 10$ [1/sec], Eq. (1) can be well approximated by the following *prompt ω -eigenvalue equation*:

$$\frac{\omega_p}{v_g} \psi_{g,p} = (-\mathbf{A} + \mathbf{F}_p) \psi_{g,p}, \quad (2)$$

where the subscript p indicates the prompt ω -mode. Consequently, α can be comparatively accurately obtained by Eq. (2) in the case of $\alpha \gg \max(\lambda_i)$.

B. Two-step Calculation Scheme for α

In this study, α was evaluated by a two-step calculation scheme, i.e. the lattice calculation by the SCALE6.2.1/NEWT [13] followed by the core calculation by the PARTISN [14]. Since measurement values of α for Cases 4~6 are $\alpha > \sim 1000$ [1/sec], the approximation using the prompt ω -eigenvalue equation is reasonable. Thus, α for Cases 4~6 are numerically analyzed on the basis of Eq. (2).

As shown in Fig. 4, two types of 2D multi-assemblies models were numerically analyzed by the NEWT to obtain 7 group homogenized cross sections for each of fuel and reflector assemblies and guide thimble for control rod. In Fig. 4, only right boundary condition is vacuum and others are reflective. These two types of models correspond to a) center and b) upper or lower core-regions, respectively. The ENDF/B-VII.1 252-group neutron library (xn252v7.1) were used in these lattice calculations. The spatial length of x -direction in the NEWT calculation was adjusted to conserve the mean chord length $l = 4V/S$ of each region in the actual 3D geometry. The spatial mesh lengths for x - and y -directions are smaller than 0.5 cm. As an angle quadrature set, a square Chebychev-Legendre set was used, where the numbers of polar and azimuthal directions are 5 and 9 per octant, respectively. The P_5 scattering was applied in all of materials. Through the lattice calculation by the NEWT, 7 group homogenized cross sections were obtained, where the collapsed 7 energy-group structure is shown in Table. I.

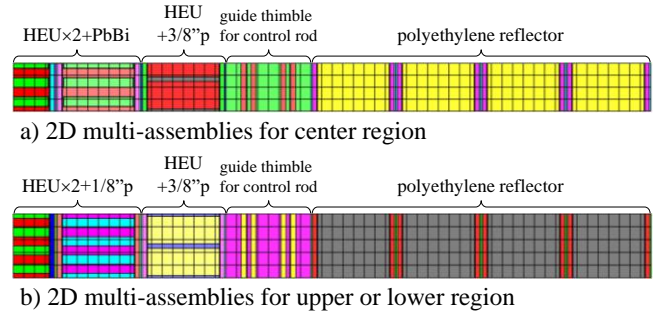


Fig. 4. Lattice calculation geometries in the NEWT.

Table I. Collapsed 7 energy-group structure

group	energy boundary [eV]	
	upper	lower
1	2.000×10^7	1.356×10^6
2	1.356×10^6	9.500×10^3
3	9.500×10^3	4.100
4	4.100	6.250×10^{-1}
5	6.250×10^{-1}	1.500×10^{-1}
6	1.500×10^{-1}	5.000×10^{-2}
7	5.000×10^{-2}	1.000×10^{-5}

Using these 7 group homogenized cross sections, the prompt ω -eigenvalue calculation in 3D core geometry was carried out by the PARTISN with the “ievt=2 (alpha search)” option. To obtain a negative value of prompt ω , or prompt neutron decay constant α , the minor modification of the PARTISN source code (tnewpa3d.f) was necessary. The validity of this modification was confirmed by comparing numerical results of α using the DANTSYS [21] with the same input files. For α search calculation, production cross section $\nu \Sigma_{f,g}$ for each fuel region was multiplied by $(1 - \beta)$ to generate prompt neutrons only, where $\beta \equiv \sum_{i=1}^6 \beta_i$ means the total delayed neutron fraction. In this study, fission spectrum χ_g were approximately treated, i.e. NEWT outputs of χ_g were just used without correction of delayed neutron spectrum. The 3D core geometry was divided by approximately $1 \times 1 \times 1$ cm meshes with 1/4 core symmetry. Instead of treating higher P_L scattering, transport cross section $\Sigma_{tr,g}$ was used. The EO₁₆ quadrature set were used as the S_N quadrature [24].

C. Random Sampling Technique for UQ of α

Once the NEWT/PARTISN analysis scheme was established, the UQ of α can be achieved by the random sampling technique [25] using the SCALE6.2.1/Sampler [10,12]. By the aid of Sampler module, random samples of homogenized cross section data, Σ_n ($n = 1 \sim 200$), were easily obtained by calling the NEWT module for each randomly sampled library data. In the Sampler procedure, the

restart file of unperturbed NEWT calculation was utilized as a first guess of neutron flux to reduce the computational time in the NEWT. In this study, total number of random sampling N was 200 because of the limitation of total calculation time.

After the Sampler/NEWT calculations, a series of PARTISN core analyses was carried out for each of random samples of homogenized cross section data Σ_n to obtain the corresponding prompt neutron decay constant α_n . Note that forward neutron flux file (rtflux) of unperturbed case was utilized as a first guess to reduce the calculation time of each PARTISN analysis. Nevertheless, compared with the k_{eff} -eigenvalue calculation, it requires longer computational time to stably obtain the converged numerical solution because of the α search algorithm. Finally, the uncertainty of α (denoted as s_α) was estimated by the square root of unbiased variance for α_n . The statistical error of s_α was estimated by the bootstrap method without assumption of normality [26,27]. As a rough estimation, if the probability distribution of α is well approximated by the normal distribution, it is expected that the relative statistical error of s_α is estimated by $1/\sqrt{2(N-1)} \approx 5\%$ in one-sigma level.

For discussion, a series of k_{eff} -eigenvalue calculations using the Sampler/NEWT/PARTISN scheme was also carried out to estimate (1) uncertainty of k_{eff} , or s_k , and (2) correlation between α and k_{eff} . By comparing the estimated s_k with that of TSUNAMI-3D, the validity of random sampling procedure was confirmed as discussed later.

IV. RESULTS

1. Uncertainty quantification of k_{eff}

Table II shows the experimental values of k_{eff} , and numerical results and uncertainties using the TSUNAMI-3D. The C/E values are approximately 1.004 for Cases 0~3, which is consistent with previous knowledge for the KUCA analyses [28]. The nuclear data-induced uncertainties $s_k = (\text{relative uncertainty}) \times k_{\text{eff}}$ are 870~880 pcm for Cases 0~6, i.e. absolute values of s_k are almost the same without depending on the subcriticality.

As an example, Fig. 5 shows the top 20 contributions of each nuclide-reaction to s_k for the critical state (Case 0) and the deepest subcritical state (Case 6). In Fig. 5, symbols ‘‘H’’ and ‘‘Al27’’ corresponds to hydrogen in polyethylene and ^{27}Al metal, respectively; words ‘‘elas.’’, ‘‘fis.’’, and ‘‘nubar’’ mean elastic scattering σ_{elas} , fission σ_f , and average number of fission-neutrons $\bar{\nu}$, respectively. For example, the value of ‘‘U235- χ ’’ indicates the contribution due to variance of ^{235}U fission spectrum χ . As another example, value of ‘‘U235-fis. vs U235-(n, γ)’’ corresponds to the contribution due to covariance between fission σ_f of ^{235}U and capture $\sigma_{(n,\gamma)}$ of ^{235}U . In the case of uncertainty of k_{eff} , major contributions are χ , $\bar{\nu}$, $\sigma_{(n,\gamma)}$, and σ_f of ^{235}U ; and $\sigma_{(n,\gamma)}$ and σ_{elas} of ^1H in polyethylene; σ_{elas} and $\sigma_{(n,n')}$ of ^{27}Al metal. On the other hand, the contributions of Pb and Bi are much smaller than

these major contributions. Thus, in order to furthermore investigate effects due to $\sigma_{(n,n')}$ of Pb and Bi, additional sample worth experiments of Pb-Bi plate are necessary in a similar way as reported Ref. [6].

Table II. Summary of k_{eff} by TSUNAMI-3D

case	k_{eff} (experiment)	k_{eff} (CE KENO-V.a)	relative uncertainty [%dk/k]
Case 0	1.00000	1.00402 \pm 0.00007	0.8669 \pm 0.0002
Case 1	0.98853 \pm 0.00005	0.99260 \pm 0.00007	0.8746 \pm 0.0002
Case 2	0.98344 \pm 0.00006	0.98757 \pm 0.00007	0.8771 \pm 0.0002
Case 3	0.97577 \pm 0.00006	0.97971 \pm 0.00007	0.8829 \pm 0.0002
Case 4		0.95758 \pm 0.00006	0.9174 \pm 0.0002
Case 5		0.91293 \pm 0.00006	0.9608 \pm 0.0002
Case 6		0.89919 \pm 0.00007	0.9766 \pm 0.0002

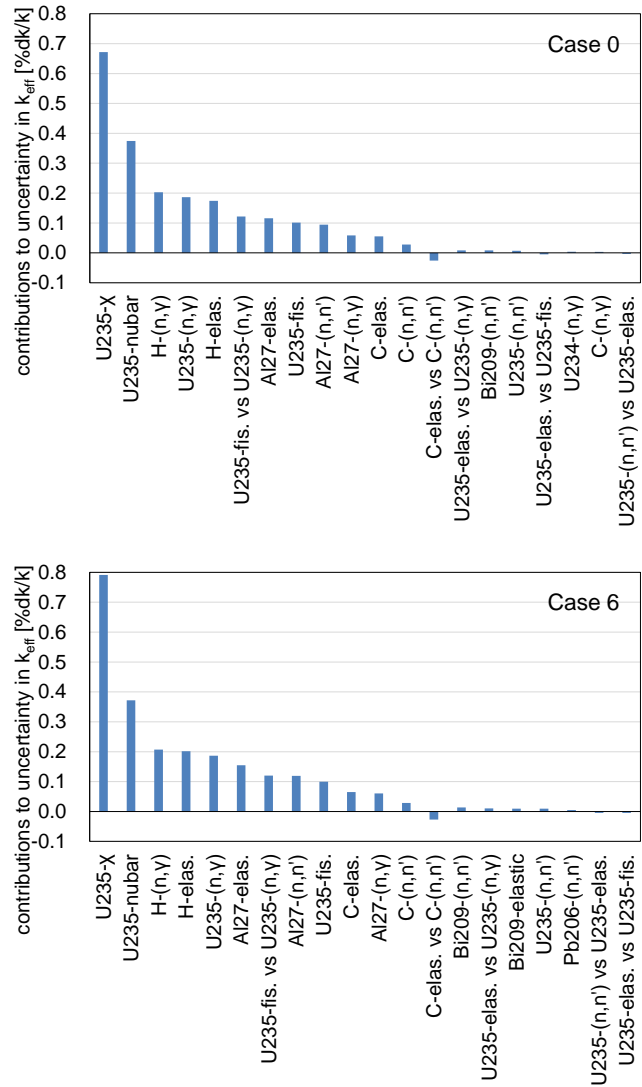


Fig. 5. Contributions of each nuclide-reaction to uncertainty

2. Uncertainty quantification of α

For Cases 4~6, Table III shows uncertainties of α and k_{eff} , or s_α and s_k , by the random sampling technique using the Sampler/NEWT/PARTISN. In Table III, bracket $[a, b]$ means 95% confidence interval estimated by the bootstrap method. The uncertainties s_k using random sampling technique are nearly equal to those of TSUNAMI-3D as shown Table II. Consequently, it is demonstrated that the random sampling scheme works well. Note that there are systematic differences (100~400 pcm) between the sample mean values of k_{eff} by the Sampler/NEWT/PARTISN and numerical results by KENO-V.a, because of the analytical modeling errors, e.g. discretization errors of space \vec{r} , energy E and direction $\vec{\Omega}$.

Table III. Summary of α and k_{eff} by the random sampling technique using Sampler/NEWT/PARTISN

	experiment fiber#2	random sampling	
		mean	uncertainty
Case 4	α [1/sec]	1022	174
	k_{eff} [-]	[998, 1046]	[158, 198]
Case 5	α [1/sec]	1770	156
	k_{eff} [-]	[1748, 1791]	[141, 176]
Case 6	α [1/sec]	1987	151
	k_{eff} [-]	[1966, 2008]	[137, 170]
		0.9541	0.0095
		[0.9528, 0.9554]	[0.0086, 0.0109]
		0.9113	0.0095
		[0.9100, 0.9126]	[0.0086, 0.0109]
		0.8984	0.0095
		[0.8971, 0.8998]	[0.0086, 0.0109]

As shown in Table III, the relative uncertainties s_α/α are 17, 9, and 8% for Cases 4, 5 and 6, respectively. In order to discuss a main factor of s_α/α , let us consider the approximate expression of α . In the one point reactor approximation, fundamental mode of eigenvalue α is expressed by

$$\alpha \approx \frac{1 - (1 - \beta_{\text{eff}})k_{\text{eff}}}{\ell} = \frac{\beta_{\text{eff}} - \rho}{\Lambda}, \quad (3)$$

where ℓ and Λ are the prompt neutron lifetime and the neutron generation time, respectively [15]. Based on the uncertainty propagation for Eq. (3), s_α/α is estimated as follows:

$$\frac{s_\alpha}{\alpha} \approx \sqrt{\begin{aligned} & \left(\frac{s_\beta}{\beta_{\text{eff}} - \rho} \right)^2 + \left(\frac{s_{-\rho}}{\beta_{\text{eff}} - \rho} \right)^2 + \left(\frac{s_\Lambda}{\Lambda} \right)^2 \\ & + 2 \left(\frac{s_\beta}{\beta_{\text{eff}} - \rho} \right) \left(\frac{s_{-\rho}}{\beta_{\text{eff}} - \rho} \right) \text{cor}(\beta_{\text{eff}}, -\rho) \\ & + 2 \left(\frac{s_\beta}{\beta_{\text{eff}} - \rho} \right) \left(\frac{s_\Lambda}{\Lambda} \right) \text{cor}(\beta_{\text{eff}}, \Lambda) \\ & + 2 \left(\frac{s_{-\rho}}{\beta_{\text{eff}} - \rho} \right) \left(\frac{s_\Lambda}{\Lambda} \right) \text{cor}(-\rho, \Lambda) \end{aligned}}, \quad (4)$$

where s_β , $s_{-\rho}$ and s_Λ are uncertainties of β_{eff} , $-\rho$ and Λ , respectively; $\text{cor}(x, y)$ is correlation coefficient between x and y . If $s_{-\rho}$ is the main factor in Eq. (4), Eq. (4) is approximated by

$$\frac{s_\alpha}{\alpha} \approx \frac{s_{-\rho}}{\beta_{\text{eff}} - \rho} \approx \frac{s_k}{k_{\text{eff}}\{1 - (1 - \beta_{\text{eff}})k_{\text{eff}}\}}, \quad (5)$$

For Cases 4~6, the estimated values of β_{eff} were approximately 0.008. Using Eq. (5) and s_k in Table II, values of $s_{-\rho}/(\beta_{\text{eff}} - \rho)$ for Cases 4~6 are 18, 10 and 9%, which are almost the same as the values of s_α/α in Table III (17, 9, and 8%). In other words, relative uncertainties of α are nearly equal to or less than those of subcriticality $-\rho$. Consequently, it is supposed that relative uncertainty $s_{-\rho}/(\beta_{\text{eff}} - \rho) \approx s_{-\rho}/(-\rho)$ is the major contribution to s_α/α .

3. Correlation between α and k_{eff}

Using the results of random samples α and k_{eff} , nuclear data-induced correlation coefficients between α and k_{eff} are estimated as shown in Table IV. From Cases 4~6 are strongly correlated to each other. In addition, the correlation coefficients between α and k_{eff} are negative, or approximately -1 . As one of the examples, Fig. 6 shows the correlation between random samples of α and k_{eff} in Case 6. Figure 6 also shows the evidence of strongly negative correlation between α and k_{eff} . The reason of negative correlation between α and k_{eff} is well explained by Eq. (3). Since α is approximately proportional to subcriticality $-\rho$, α tends to be larger as k_{eff} decreases. By differentiating Eq. (3) with respect to a cross section σ , the following relationship is obtained:

$$\ell \frac{d\alpha}{d\sigma} \approx k_{\text{eff}} \frac{d\beta_{\text{eff}}}{d\sigma} - (1 - \beta_{\text{eff}}) \frac{dk_{\text{eff}}}{d\sigma} - \alpha \frac{d\ell}{d\sigma}, \quad (6)$$

Thus, the gradient of $dk_{\text{eff}}/d\alpha \approx -60$ [μsec] in Fig. 6 approximately corresponds to $-\ell$.

Table IV. Nuclear data-induced correlation coefficients among α and k_{eff} for Cases 4~6

	α			k_{eff}			
	Case 4	Case 5	Case 6	Case 4	Case 5	Case 6	
α	Case 4	1.000	0.999	0.997	-0.998	-0.998	-0.997
	Case 5	0.999	1.000	1.000	-0.994	-0.994	-0.994
	Case 6	0.997	1.000	1.000	-0.992	-0.992	-0.992
k_{eff}	Case 4	-0.998	-0.994	-0.992	1.000	1.000	0.999
	Case 5	-0.998	-0.994	-0.992	1.000	1.000	1.000
	Case 6	-0.997	-0.994	-0.992	0.999	1.000	1.000

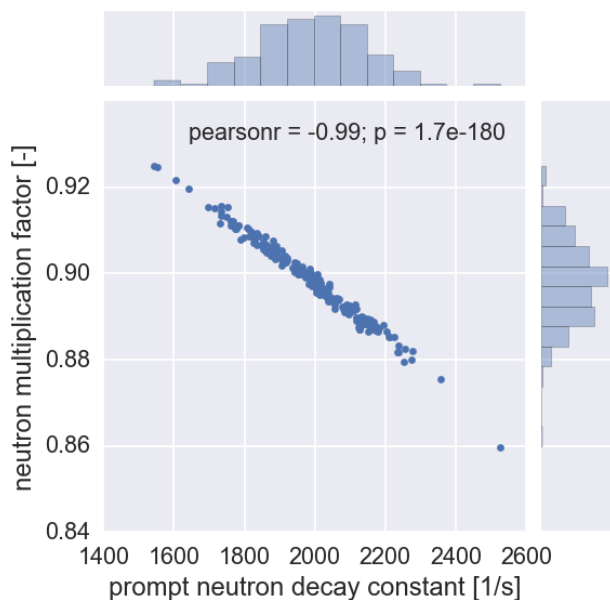


Fig. 6 Correlation between random samples of α and k_{eff} with these histograms (Case 6).

The correlation between α and k_{eff} implies that numerical prediction values of k_{eff} can be improved by a data assimilation technique using measurement values of α for subcritical systems. Examples of the data assimilation techniques are the bias factor method [29] and cross section adjustment technique [30]. As discussed in Ref. [29], measurement values, which have strong correlation with target parameters, are very useful information to reduce the uncertainties of predicted target values. One of the future tasks is application of the data assimilation technique using measured α to precisely predict k_{eff} .

V. CONCLUSIONS

In this paper, nuclear data-induced uncertainties of neutron multiplication factor k_{eff} and prompt neutron decay constant α for the Pb-Bi loaded ADS experiments at KUCA. As the analytical tool for SA and UQ of k_{eff} , the SCALE6.2.1/TSUNAMI-3D was utilized. In the case of this experiment, contributions of Pb and Bi to uncertainty of k_{eff} are much smaller than other contributions such as nuclear data of ^{235}U , ^1H and ^{27}Al . On the other hand, the analytical tool for UQ of α is not yet put into practical use. As one of the feasibility studies, UQ of α using the random sampling technique was investigated for two-step (lattice-core) calculation scheme. This random sampling is achieved by the SCALE6.2.1/Sampler module. Consequently, it is supposed that the nuclear data-induced uncertainty of subcriticality is major contribution to the uncertainty of α . Furthermore, as expected from the theoretical relationship between α and k_{eff} , it is confirmed that the nuclear data-induced correlation between them is strongly negative. This fact implies that the

numerical prediction value of k_{eff} can be improved by the data assimilation technique using subcritical experimental results such as α .

ACKNOWLEDGEMENT

This work is supported under the project of *Basic Research for Nuclear Transmutation Techniques by Accelerator-Driven System*, a Special Research Program funded by Chubu Electric Power Co., Inc. The authors are grateful to all the staff at KUCA and to the FFAG accelerator group for their assistance during the experiments.

REFERENCES

1. C.H. PYEON, T. MISAWA, J.Y. LIM, et al., "First Injection of Spallation Neutrons Generated by High-Energy Protons into the Kyoto University Critical Assembly," *J. Nucl. Sci. Technol.*, 46, 1091 (2009).
2. C.H. PYEON, H. SHIGA, K. ABE, et al., "Reaction Rate Analysis of Nuclear Spallation Reactions Generated by 150, 190, and 235MeV Protons," *J. Nucl. Sci. Technol.*, 47, 1090 (2010).
3. J.Y. LIM, C.H. PYEON, T. YAGI, et al., "Subcritical Multiplication Parameters of the Accelerator-Driven System with 100 MeV Protons at the Kyoto University Critical Assembly," *Sci. Technol. Nucl. Install.*, 2012, Article ID: 395878 (2012).
4. C.H. PYEON, T. AZUMA, Y. TAKEMOTO, et al., "Experimental Analyses of Spallation Neutrons Generated by 100 MeV Protons at the Kyoto University Critical Assembly," *Nucl. Eng. Technol.*, 45, 81 (2013).
5. C.H. PYEON, H. NAKANO, M. YAMANAKA, et al., "Neutron Characteristics of Solid Targets in Accelerator-Driven System with 100-MeV Protons at Kyoto University Critical Assembly," *Nucl. Technol.*, 192, 181 (2015).
6. C.H. PYEON, A. FUJIMOTO, T. SUGAWARA, et al., "Validation of Pb Nuclear Data by Monte Carlo Analyses of Sample Reactivity Experiments at Kyoto University Critical Assembly," *J. Nucl. Sci. Technol.*, 53, 602 (2016).
7. C.H. PYEON, M. YAMANAKA, Y. TAKAHASHI, "Experimental Benchmarks on Subcriticality in Accelerator-Driven System with 100 MeV Protons at Kyoto University Critical Assembly," *Proc. of PHYSOR2016*, Sun Valley, Idaho, May 1-5, 2016, American Nuclear Society (2016).
8. J.-B. LAGRANGE, T. PLANCHE, E. YAMAKAWA, et al., "Straight Scaling FFAG Beam Line," *Nucl. Instrum. Methods A*, 691, 55 (2012).
9. E. YAMAKAWA, T. UESUGI, J.-B. LAGRANGE, et al., "Serpentine Acceleration in Zero-chromatic FFAG Accelerators," *Nucl. Instrum. Methods A*, 716, 46. (2013).

10. B.T. REARDEN, M.A. JESSEE, "SCALE Code System," ORNL/TM-2005/39 Version 6.2.1, Oak Ridge National Laboratory (2016).
11. C.M. PERFETTI, "Advanced Monte Carlo Methods for Eigenvalue Sensitivity Coefficient Calculation," doctoral dissertation, University of Michigan (2012).
12. M.L. WILLIAMS, G. ILAS, M.A. JESSEE, et al., "A Statistical Sampling Method for Uncertainty Analysis with SCALE and XSUSA," *Nucl. Technol.*, 183, 515 (2013).
13. M.D. DEHART, "Advancements in Generalized-Geometry Discrete Ordinates Transport for Lattice Physics Calculations," *Proc. of PHYSOR-2006*, Vancouver, Canada, September 10-14, 2006, American Nuclear Society. (2006).
14. R.E. ALCOUFFE, R.S. BAKER, J.A. DAHL, et al., "PARTISN: A Time-Dependent, Parallel Neutral Particle Transport Code System," LA-UR-08-07258, Los Alamos National Laboratory (2008).
15. T. MISAWA, H UNESAKI, C.H. PYEON, *Nuclear Reactor Physics Experiments*, Kyoto University Press, Japan (2010).
16. J.T. GOORLEY, M.R. JAMES, T.E. BOOTH, et al., "Initial MCNP6 Release Overview - MCNP6 version 1.0," LA-UR-13-22934, Los Alamos National Laboratory (2013).
17. K. SHIBATA, O. IWAMOTO, T. NAKAGAWA, et al., "JENDL-4.0: A New Library for Nuclear Science and Engineering," *J Nucl. Sci. Technol.*, 48, 1, (2011).
18. T. YAGI, C.H. PYEON, T. MISAWA, "Application of Wavelength Shifting Fiber to Subcriticality Measurements," *Appl. Radiat. Isot.*, 72, 11 (2013).
19. S. GOLUOGLU, M.E. DUNN, L.M. PETRIE, et al., "Development and Validation of the New Continuous-Energy Capability in the Criticality Safety Code in KENO," *Proc. of PHYSOR2008*, Interlaken, Switzerland, September 14-19, 2008, Paul Scherrer Institut (2008).
20. M.B. CHADWICK, M. HERMAN, P. OBLOŽINSKÝ, et al., "ENDF/B-VII.1 Nuclear Data for Science and Technology: Cross Sections, Covariances, Fission Product Yields and Decay Data," *Nucl. Data Sheets*, 112, 2887 (2011).
21. R.E. ALCOUFFE, R.S. BAKER, F.W. BRINKLEY, et al., "DANTSYS: A Diffusion Accelerated Neutral Particle Transport Code System," LA-12969-M, Oak Ridge National Laboratory (1995).
22. A.F. HENRY, "The Application of Inhour Modes to the Description of Non-Separable Reactor Transients," *Nucl. Sci. Eng.*, 20, 338 (1964).
23. W.M. STACY, *Space-time Nuclear Reactor Kinetics*, Academic Press, New York (1969).
24. T. ENDO, A. YAMAMOTO, "Development of New Solid Angle Quadrature Sets to Satisfy Even- and Odd-Moment Conditions," *J. Nucl. Sci. Technol.*, 44, 1249 (2007).
25. A. YAMAMOTO, K. KINOSHITA, T. WATANABE, et al., "Uncertainty Quantification of LWR Core Characteristics Using Random Sampling Method," *Nucl. Sci. Eng.*, 181, 160 (2015).
26. B. EFRON, "Bootstrap Methods: Another Look at the Jackknife," *Ann. Stat.*, 7, 1 (1979).
27. T. ENDO, T. WATANABE, A. YAMAMOTO, "Confidence Interval Estimation by Bootstrap Method for Uncertainty Quantification Using Random Sampling Method," *J. Nucl. Sci. Technol.*, 52, 993 (2015).
28. J. CHRISTENSEN, K. TONOIKE, J.D. BESS, et al., "Evaluation of the Kyoto University Critical Assembly Erbium Oxide Experiments," ICSBEP, NEA/NSC/DOC/(95)03/IV, LEU-MET-THERM-005, NEA (2012).
29. T. ENDO, A. YAMAMOTO, T. WATANABE, "Bias Factor Method Using Random Sampling Technique," *J. Nucl. Sci. Technol.*, 53, 1494 (2016).
30. T. WATANABE, T. ENDO, A. YAMAMOTO, et al., "Cross Section Adjustment Method Based on Random Sampling Technique," *J. Nucl. Sci. Technol.*, 51, 590 (2014).